Supplementary Information

Free-standing polydopamine films generated in the presence of different metallic ions: the comparison of reaction process and film properties

Xuwen Han, Feng Tang and Zhaoxia Jin*

Department of Chemistry, Renmin University of China

Beijing, 100872

Peoples Republic of China

Contents

Table S1. The purity and the contents of main impurity in four salts used.

Composition at. (≥ %)		Impurities (≤ %)		
		Mg	Ca	Fe
NaCl (AR)	99.5	0.002	0.005	0.0002
MgCl2•6H_2O (AR)	98.0	~	0.05	0.0005
$CaCl_2$ (AR)	96.0	0.3	~	0.001
$CoCl_2$•6H_2O (CP)	99.99	~	~	~

Table S2. The contents of different metallic elements (at.%) in polydopamine films and nanoparticles obtained through ICP-OES.

Molar percentage	Na in Na-PDA	Mg in Mg-PDA	Ca in Ca-PDA	Co in Co-PDA
film	7.35%	1.31%	2.56%	0.20%
nanoparticles	8.59%	1.06%	2.22%	0.16%

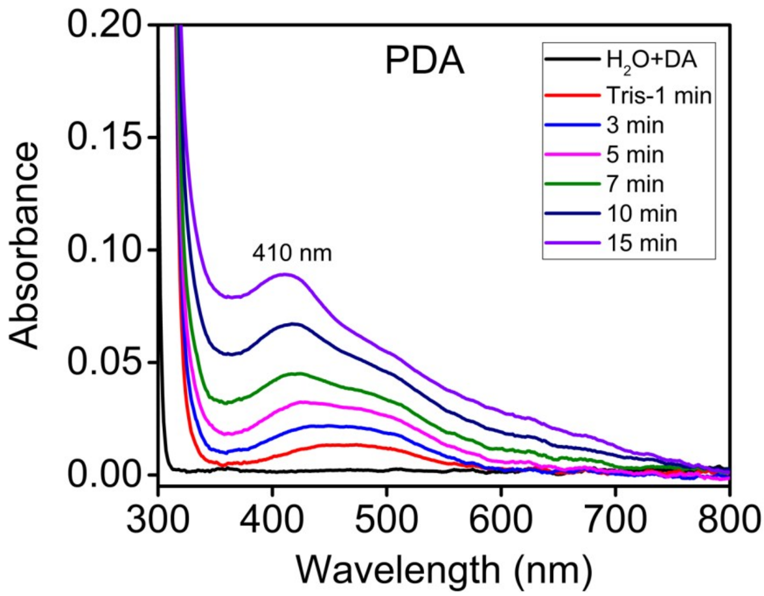

Figure S1. UV-vis spectra of oxidative polymerization of dopamine (10 mM) in the addition of Tris buffer (10 mM, pH = 8.8).

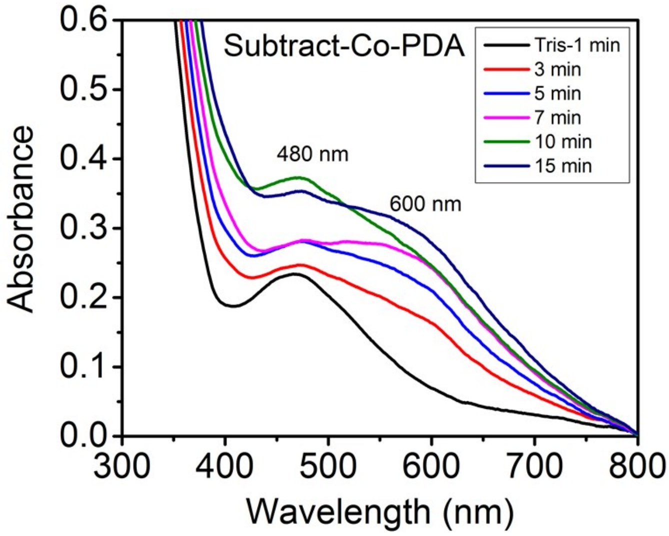

Figure S2. UV-vis spectra of oxidative polymerization of dopamine (10 mM) in the presence of Co^{2+} (100 mM) in which the absorption spectrum of Co^{2+} was subtracted.

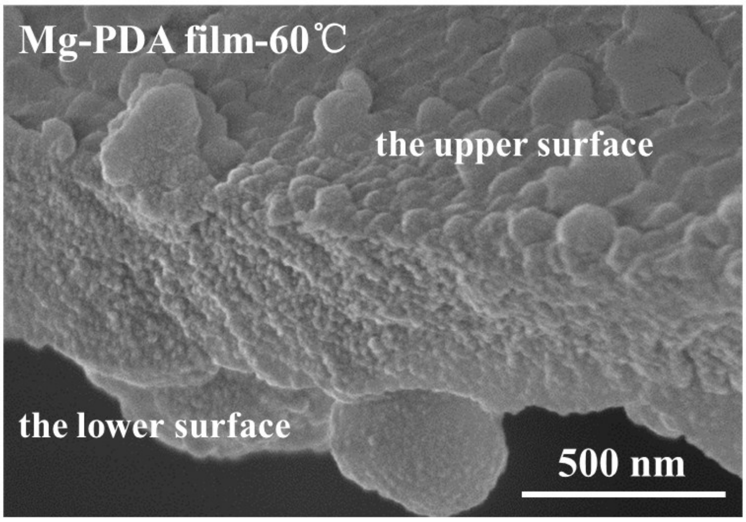

Figure S3. SEM images of rugged Mg-PDA film formation at 60 °C for 2 days. The concentration of dopamine was 10 mM, while the concentration for Mg^{2+} metal ions was 100 mM.

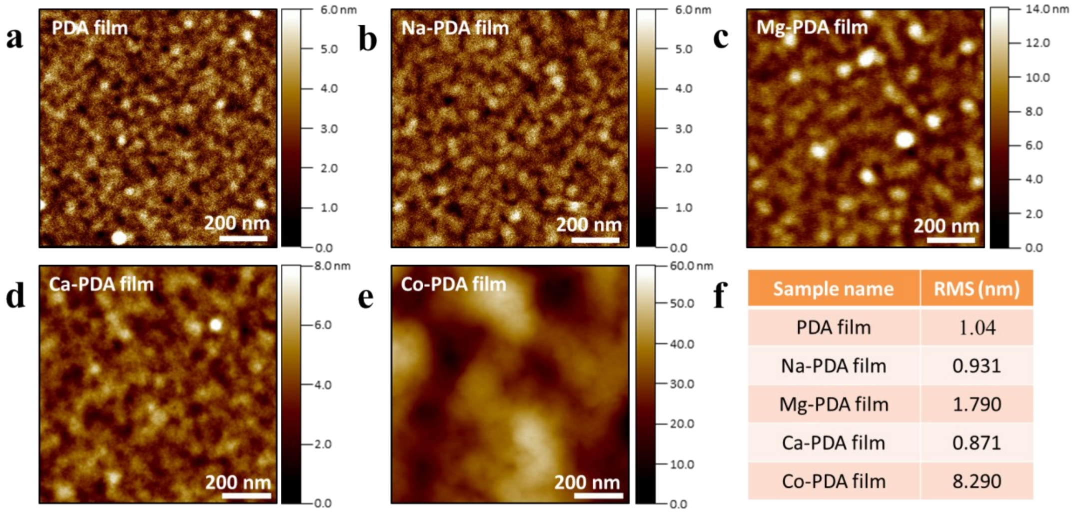

Sample name	RMS (nm)
PDA film	1.04
Na-PDA film	0.931
Mg-PDA film	1.790
Ca-PDA film	0.871
Co-PDA film	8.290

Figure S4. AFM images of PDA films generated in different conditions after reaction of 150 minutes. (a) Without salt. (b) With NaCl (100 mM). (c) With $MgCl_2$ (100 mM). (d) With $CaCl_2$ (100 mM). (e) With $CoCl_2$ (100 mM). (f) Root mean roughness (RMS) of these PDA films.

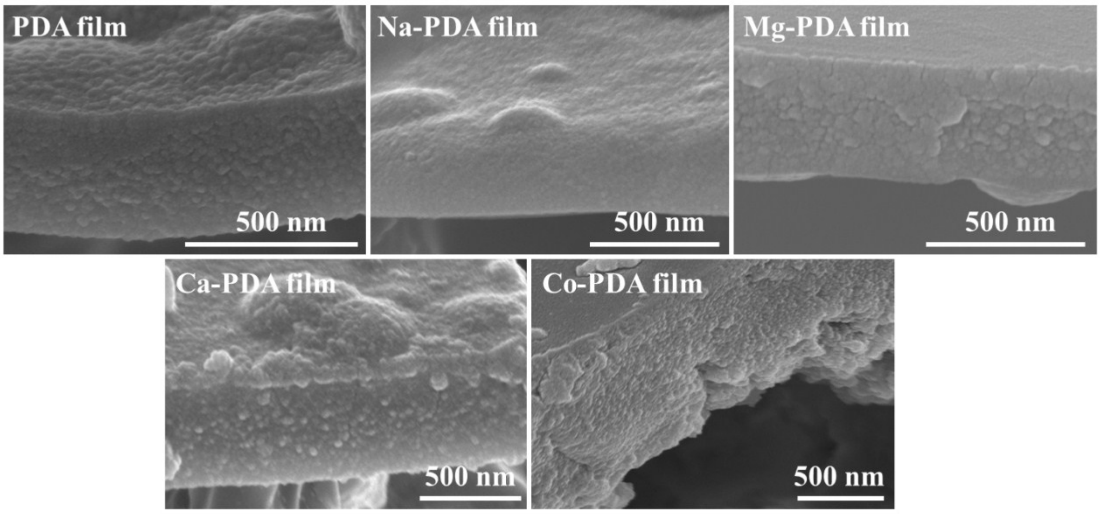

Figure S5. SEM images of PDA films generated in different conditions after reaction of 20 days, cross-section of films shown their thickness.

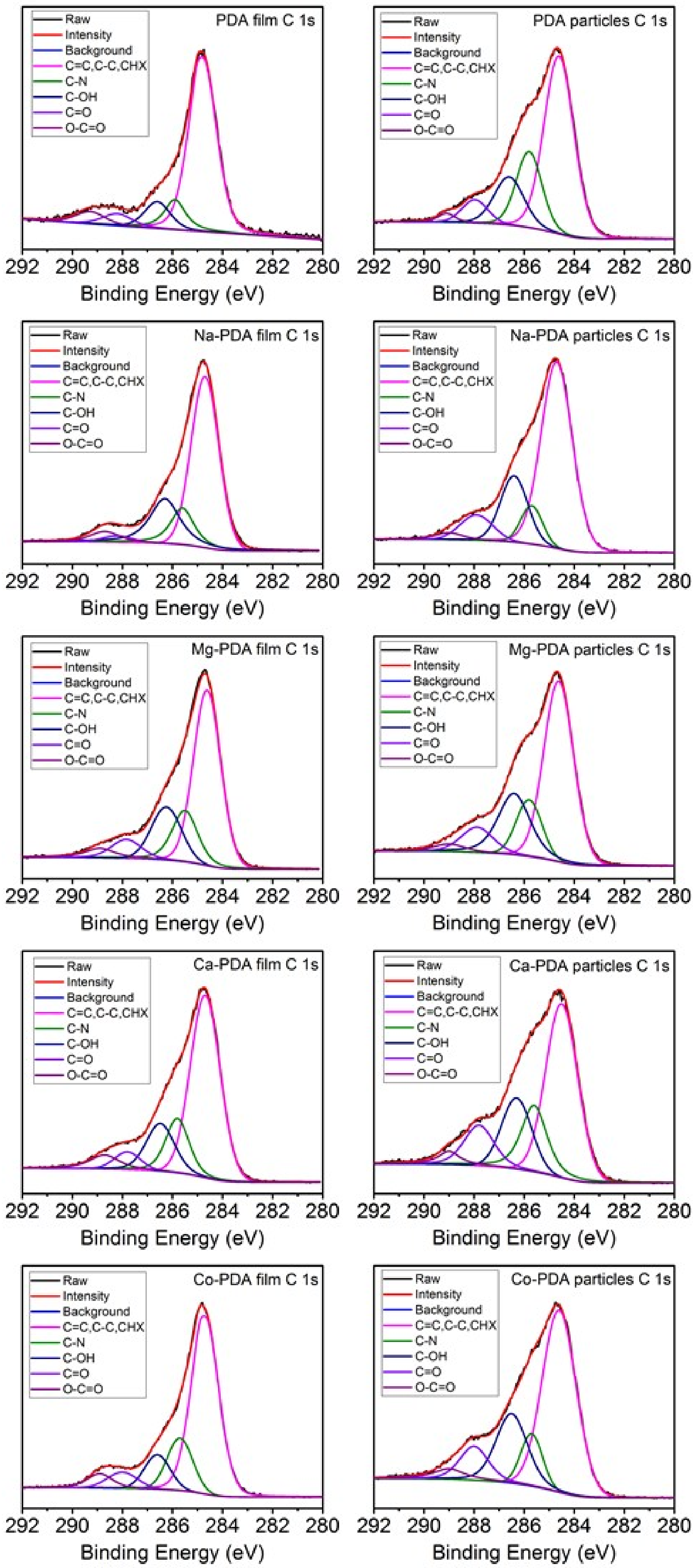
PDA film C 1s
PDA particles C 1s
Na-PDA film C 1s
Na-PDA particles C 1s
Mg-PDA film C 1s
Mg-PDA particles C 1s
Ca-PDA film C 1s
Ca-PDA particles C 1s
Co-PDA film C 1s
Co-PDA particles C 1s
Raw
Intensity
Background
C=C,C-C,CHX
C-N
C-OH
C=O
O-C=O
292 290 288 286 284 282 280
Binding Energy (eV)

Figure S6. The high-resolution XPS spectra of the C1s core-level for PDA-Na, PDA-Mg, PDA-Ca and PDA-Co film samples were compared with pristine PDA films.

Table S3. The detailed component in C1s of polydopamine films and nanoparticles generated in different conditions.

samples		C1s				
		C=C, C-C	C-N	C-OH	C=O	-O-C=O
PDA	film	67.9	11.2	9.9	5.4	5.5
	NPs	55.5	20.9	15.4	6.3	1.9
PDA-Na	film	57.6	13.9	21.6	2.3	4.6
	NPs	61.9	8.5	18.8	8.4	2.5
PDA-Mg	film	54.1	17.0	17.4	7.0	4.4
	NPs	54.2	13.9	22.2	8.7	2.8
PDA-Ca	film	58.1	15.5	15.5	5.0	5.8
	NPs	47.9	18.3	18.2	11.9	3.6
PDA-Co	film	62.7	16.0	10.5	5.7	5.2
	NPs	54.7	10.0	21.1	9.9	4.3

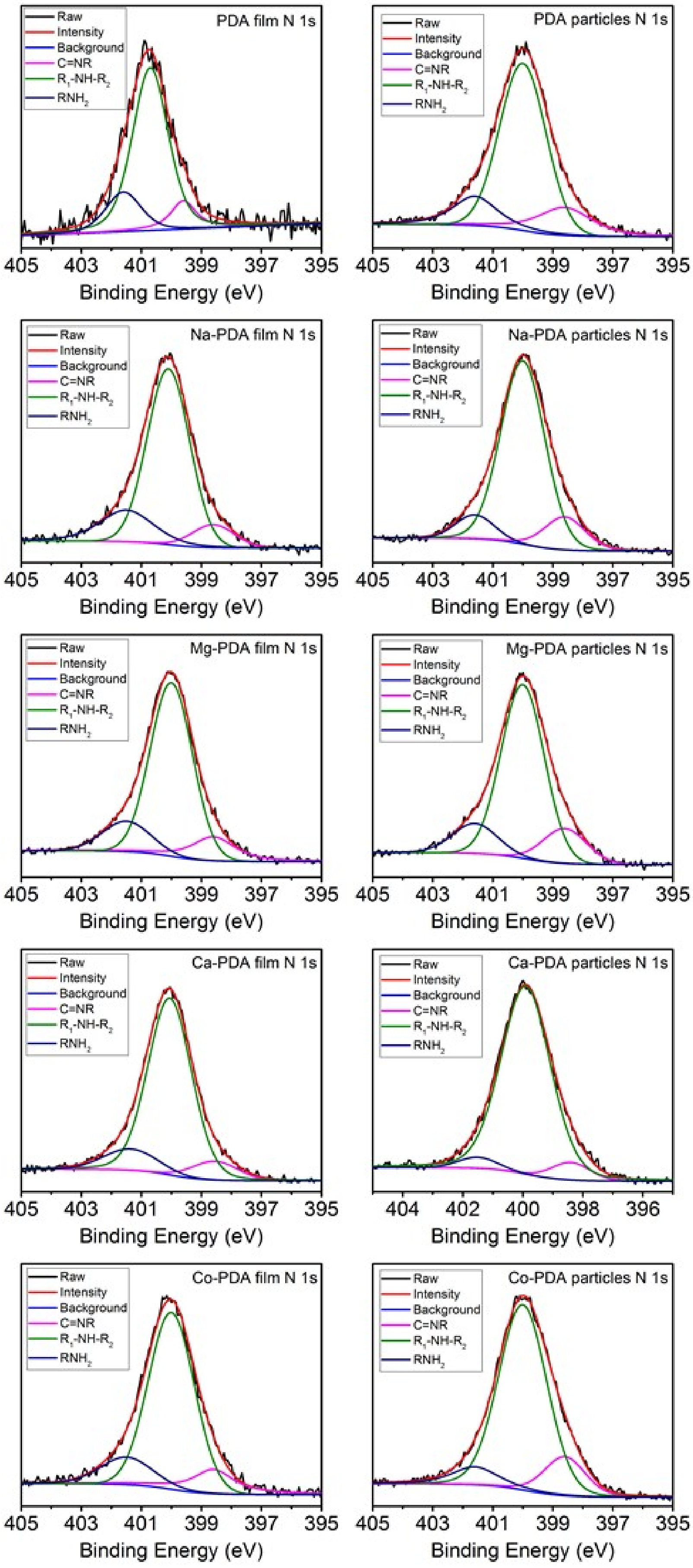
PDA film N 1s
Raw
Intensity
Background
C=NR
R1-NH-R2
RNH2
405 403 401 399 397 395
Binding Energy (eV)
PDA particles N 1s
Raw
Intensity
Background
C=NR
R1-NH-R2
RNH2
405 403 401 399 397 395
Binding Energy (eV)
Na-PDA film N 1s
Raw
Intensity
Background
C=NR
R1-NH-R2
RNH2
405 403 401 399 397 395
Binding Energy (eV)
Na-PDA particles N 1s
Raw
Intensity
Background
C=NR
R1-NH-R2
RNH2
405 403 401 399 397 395
Binding Energy (eV)
Mg-PDA film N 1s
Raw
Intensity
Background
C=NR
R1-NH-R2
RNH2
405 403 401 399 397 395
Binding Energy (eV)
Mg-PDA particles N 1s
Raw
Intensity
Background
C=NR
R1-NH-R2
RNH2
405 403 401 399 397 395
Binding Energy (eV)
Ca-PDA film N 1s
Raw
Intensity
Background
C=NR
R1-NH-R2
RNH2
405 403 401 399 397 395
Binding Energy (eV)
Ca-PDA particles N 1s
Raw
Intensity
Background
C=NR
R1-NH-R2
RNH2
404 402 400 398 396
Binding Energy (eV)
Co-PDA film N 1s
Raw
Intensity
Background
C=NR
R1-NH-R2
RNH2
405 403 401 399 397 395
Binding Energy (eV)
Co-PDA particles N 1s
Raw
Intensity
Background
C=NR
R1-NH-R2
RNH2
405 403 401 399 397 395
Binding Energy (eV)

Figure S7. The high-resolution XPS spectra of the N1s core-level for PDA-Na, PDA-Mg, PDA-Ca and PDA-Co film samples were compared with pristine PDA films.

Table S4. The detailed component in N1s of polydopamine films and nanoparticles generated in different conditions.

samples		N1s		
		C=NR	R_1-NH-R_2	RNH_2
PDA	film	11.1	71.3	17.5
	NPs	16.8	68.2	15.0
PDA-Na	film	9.3	71.7	19.0
	NPs	13.6	77.8	8.6
PDA-Mg	film	13.5	72.0	14.5
	NPs	14.6	72.0	13.4
PDA-Ca	film	8.4	80.4	11.2
	NPs	6.1	90.1	3.7
PDA-Co	film	13.6	72.6	13.8
	NPs	14.4	76.8	8.8

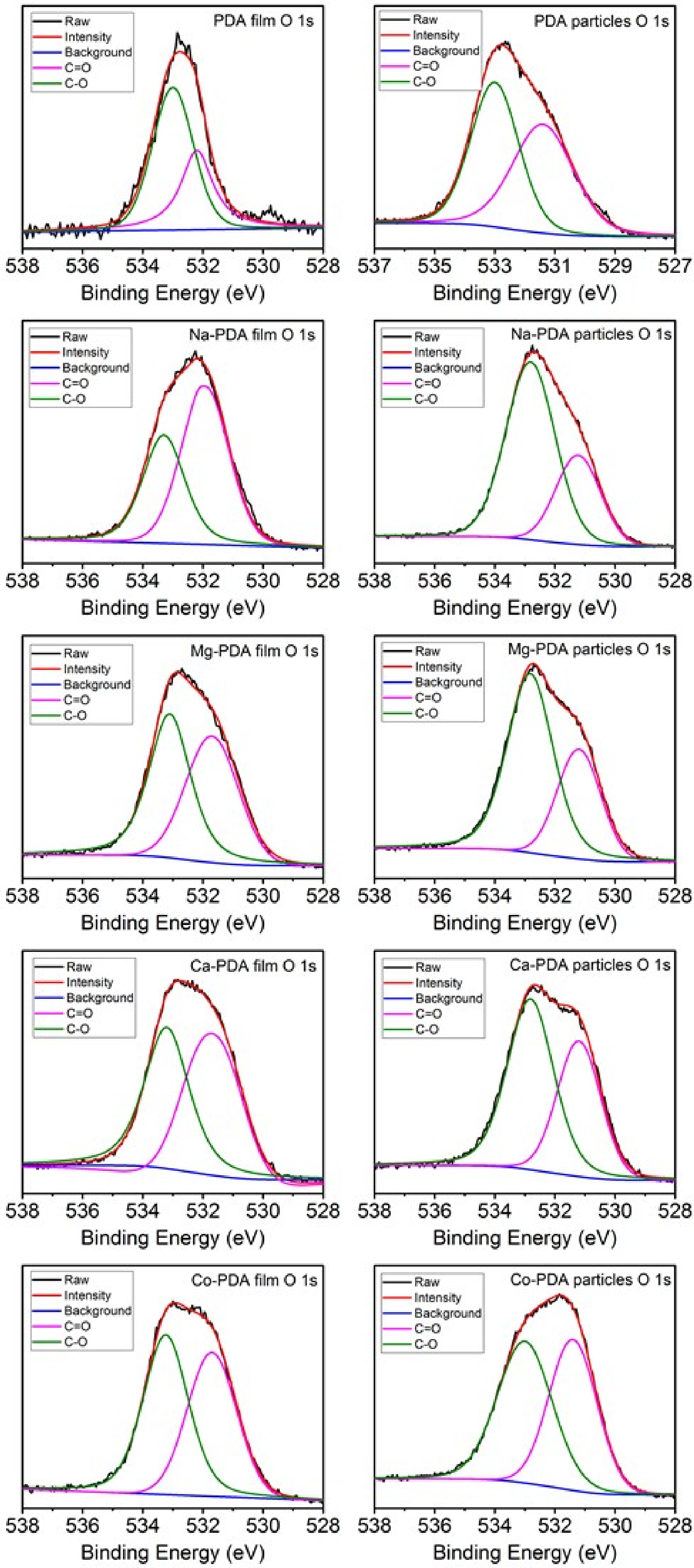

PDA film O 1s
PDA particles O 1s
Na-PDA film O 1s
Na-PDA particles O 1s
Mg-PDA film O 1s
Mg-PDA particles O 1s
Ca-PDA film O 1s
Ca-PDA particles O 1s
Co-PDA film O 1s
Co-PDA particles O 1s
Raw
Intensity
Background
C=O
C-O
Binding Energy (eV)
538
536
534
532
530
528
537
535
533
531
529
527

Figure S8. The high-resolution XPS spectra of the O1s core-level for PDA-Na, PDA-Mg, PDA-Ca and PDA-Co film samples were compared with pristine PDA films.

Table S5. The detailed component in O1s of polydopamine films and nanoparticles generated in different conditions.

samples		O1s	
		C=O	C-O
PDA	film	37.3	62.7
	NPs	49.3	50.7
PDA-Na	film	61.6	38.4
	NPs	30.1	69.9
PDA-Mg	film	47.0	53.0
	NPs	33.5	66.5
PDA-Ca	film	44.6	55.4
	NPs	40.1	59.9
PDA-Co	film	46.3	53.7
	NPs	46.7	53.3

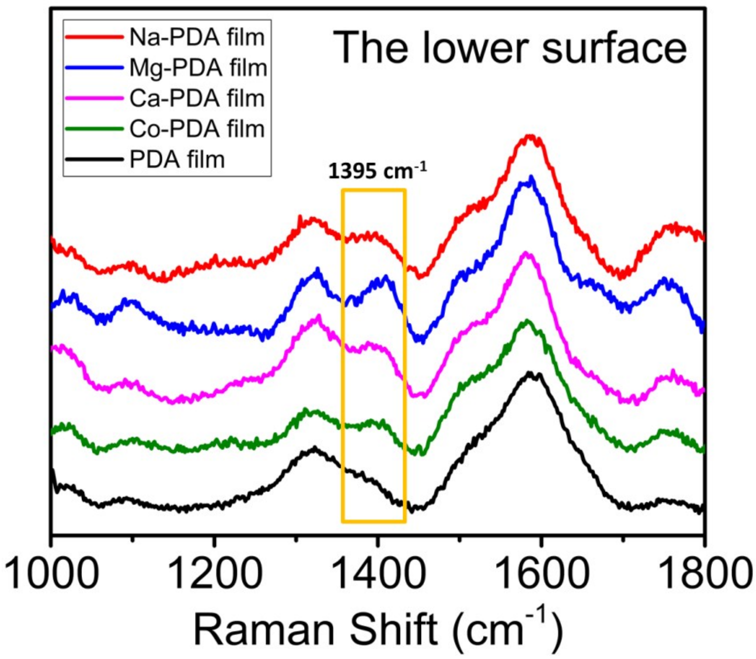

Figure S9. Raman spectra of the lower surface of PDA films generated in salty conditions.

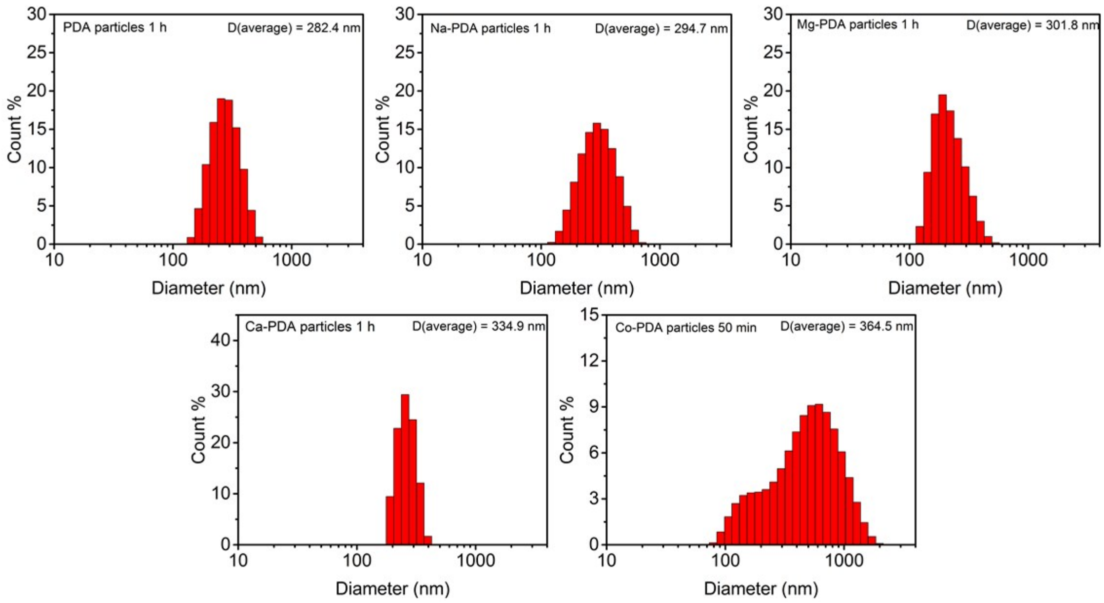

Figure S10. DLS of PDA nanoparticles in the suspension of different systems after 1 h reaction.